

Adaptation of the Aerospace Near-Infrared Imaging Spectrograph for Observation of Rocket Launches

20 May 2004

Prepared by

R. J. RUDY, R. H. FUJINO, S. M. MAZUK, W. J. SKINNER,
C. VENTURINI, and R. M. YOUNG
Space Science Applications Laboratory
Laboratory Operations

D. W. WARREN
Sensor Systems Subdivision

Prepared for

SPACE AND MISSILE SYSTEMS CENTER
AIR FORCE SPACE COMMAND
2430 E. El Segundo Boulevard
Los Angeles Air Force Base, CA 90245

Engineering and Technology Group

APPROVED FOR PUBLIC RELEASE;
DISTRIBUTION UNLIMITED

BEST AVAILABLE COPY

This report was submitted by The Aerospace Corporation, El Segundo, CA 90245-4691, under Contract No. FA8802-04-C-0001 with the Space and Missile Systems Center, 2430 E. El Segundo Blvd., Los Angeles Air Force Base, CA 90245. It was reviewed and approved for The Aerospace Corporation by J. A. Hackwell, Principal Director, Space Science Applications Laboratory; and I. Ghozeil, Principal Director, Sensor Systems Subdivision. Michael Zambrana was the project officer for the Mission-Oriented Investigation and Experimentation (MOIE) program.

This report has been reviewed by the Public Affairs Office (PAS) and is releasable to the National Technical Information Service (NTIS). At NTIS, it will be available to the general public, including foreign nationals.

This technical report has been reviewed and is approved for publication. Publication of this report does not constitute Air Force approval of the report's findings or conclusions. It is published only for the exchange and stimulation of ideas.

A handwritten signature in cursive script, reading "Michael Zambrana", written in dark ink. The signature is fluid and stylized, with the first and last names being clearly legible.

Michael Zambrana
SMC/AXE

REPORT DOCUMENTATION PAGE				Form Approved OMB No. 0704-0188	
Public reporting burden for this collection of information is estimated to average 1 hour per response, including the time for reviewing instructions, searching existing data sources, gathering and maintaining the data needed, and completing and reviewing this collection of information. Send comments regarding this burden estimate or any other aspect of this collection of information, including suggestions for reducing this burden to Department of Defense, Washington Headquarters Services, Directorate for Information Operations and Reports (0704-0188), 1215 Jefferson Davis Highway, Suite 1204, Arlington, VA 22202-4302. Respondents should be aware that notwithstanding any other provision of law, no person shall be subject to any penalty for failing to comply with a collection of information if it does not display a currently valid OMB control number. PLEASE DO NOT RETURN YOUR FORM TO THE ABOVE ADDRESS.					
1. REPORT DATE (DD-MM-YYYY) 20-05-2004		2. REPORT TYPE		3. DATES COVERED (From - To)	
4. TITLE AND SUBTITLE Adaptation of the Aerospace Near-Infrared Imaging Spectrograph for Observations of Rocket Plumes				5a. CONTRACT NUMBER FA8802-04-C-0001	
				5b. GRANT NUMBER	
				5c. PROGRAM ELEMENT NUMBER	
6. AUTHOR(S) R. J. Rudy, R. H. Fujino, S. M. Mazuk, W. J. Skinner, C. C. Venturini, R. M. Young, and D. W. Warren				5d. PROJECT NUMBER	
				5e. TASK NUMBER	
				5f. WORK UNIT NUMBER	
7. PERFORMING ORGANIZATION NAME(S) AND ADDRESS(ES) The Aerospace Corporation Laboratory Operations El Segundo, CA 90245-4691				8. PERFORMING ORGANIZATION REPORT NUMBER TR-2004(8570)-3	
9. SPONSORING / MONITORING AGENCY NAME(S) AND ADDRESS(ES) Space and Missile Systems Center Air Force Space Command 2450 E. El Segundo Blvd. Los Angeles Air Force Base, CA 90245				10. SPONSOR/MONITOR'S ACRONYM(S) SMC	
				11. SPONSOR/MONITOR'S REPORT NUMBER(S) SMC-TR-04-16	
12. DISTRIBUTION/AVAILABILITY STATEMENT Approved for public release; distribution unlimited.					
13. SUPPLEMENTARY NOTES					
14. ABSTRACT This document describes the auxiliary equipment used to adapt the Aerospace Near-Infrared Imaging Spectrograph (NIRIS) for remote sensing and the specific configuration used for launch observations at Vandenberg AFB. This equipment enables NIRIS's considerable capability for hyperspectral imaging and absolute spectrophotometry (including instantaneous wavelength coverage from 0.8-2.5 μ m at spectral resolutions from 560-1200) to be applied to a number of remote sensing observations, but most specifically the spatially resolved spectroscopy of rocket plumes. Equipment includes a small telescope that provides a 9° field of view in the spatial dimension (along the slit), digital cameras for both slit viewing and direct imaging of the field, a fast shutter and filterwheel outfitted with neutral density filters for brightness control and saturation avoidance, and an electrically isolating interface plate that allows mounting the entire 400+ lb package to a large alt-azimuth tracking mount.					
15. SUBJECT TERMS Remote Sensing, Hyperspectral Imaging, Infrared Instrumentation					
16. SECURITY CLASSIFICATION OF:			17. LIMITATION OF ABSTRACT	18. NUMBER OF PAGES 23	19a. NAME OF RESPONSIBLE PERSON
a. REPORT UNCLASSIFIED	b. ABSTRACT UNCLASSIFIED	c. THIS PAGE UNCLASSIFIED			19b. TELEPHONE NUMBER (include area code) Richard Rudy (310) 336-5799

Acknowledgments

We wish to thank D. J. Mabry for help with the data acquisition system, S. Nuygen for help in interfacing the equipment on the tracking mount, and Dr. J. Barrie for fabricating the neutral density filters. Stan Fujioka provided logistical support at VAFB. Bruce Richards, Chris Wiant, and Jim Bauer were the tracking mount operators and were essential in collecting the actual observations. Dr. Bill Dimpfl organized the Vandenberg operations and supported their execution. Dr. Paul Zittel provided crucial estimates of plume intensities prior to launch and a careful analysis of the observations afterwards that led to improvements in the experimental equipment. This work was supported by the US Air Force Space and Missile Systems Center through the Mission Oriented Investigation and Experimentation program, under contract F4701-00-C-0009.

Contents

1. Background	1
2. The Foreoptics.....	3
3. Mechanical Design	7
4. Electronics and Data acquisition	11
5. Supplementary Imaging.....	13
6. Calibration.....	17
7. Performance Capabilities.....	19
8. Summary and Future Upgrades.....	21

Figures

1. 9° FOV telescope that serves as the foreoptic for the NIRIS spectrograph.....	5
2. Cut-away view of the telescope demonstrating its function	5
3. The NIRIS spectrograph (gold structure) together with the supporting equipment used to adapt NIRIS for hyperspectral imaging of rocket plumes.....	7
4. A second view of the instrument setup	8
5. Simplified scale drawing of cine-sextant mount with NIRIS spectrograph	8
6. The NIRIS spectrograph installed on the Photo-Sonics cine sextant tracking mount as it is being towed to its observing site at Vandenberg Air Force Base.....	9
7. Block diagram showing the key experimental equipment, the control and data acquisition computers, and the connectivity among the components.....	11
8. Image from the slit viewing.....	13
9. Titan II DMSP Launch from October 18, 2003 at Vandenberg Air Force.....	14
10. Image of Titan II DMSP from 25 s after liftoff.	15

11. Image of Titan II DMSP from 90 s after liftoff.....	15
12. Spectrum of the bright infrared star α Orionis acquired shortly before sunrise on the morning of Oct 18, 2003 from Vandenberg Air Force Base.....	20
13. Spectrum of sunlit sky from shortly after the Titan II NOAA launch.....	20

Tables

1. Code V Description of NIRIS Foreoptic	4
2. Summary of Instrument Parameters and Capabilities	19

1. Background

The Aerospace Near-Infrared Imaging Spectrograph (NIRIS) is a long-slit spectrograph that covers the wavelength range 0.8–2.5 μm at a spectral resolution $\lambda/\Delta\lambda$ that can vary between 560–1200 depending on wavelength and slit width. It does this by using two 1024 x 512 HgCdTe focal-plane arrays (FPAs), fed by two cameras, two gratings, and two collimators. A common slit and field lens ensure that both “channels” of this spectrograph view the same field; a beamsplitter that switches from reflection to transmission at 1.38 μm separates the “blue” (0.8–1.4 μm) and the “red” (1.4–2.5 μm) channels. NIRIS was designed primarily for astronomical research, but it was desirable to make use of its considerable capability for a variety of remote sensing programs. These included observations of a number of rocket plumes associated with launches from Vandenberg Air Force Base (VAFB). To adapt NIRIS from the very low light astronomical observations for which it was originally designed to observations of very bright targets (that were sometimes viewed during full day-light) involved a number of adaptations that are described below.

2. The Foreoptics

As noted in the previous section, NIRIS is an imaging spectrograph. That is, an image that is projected on its entrance aperture (a 33-mm-long slit) is spectrally dispersed and reimaged on its two 2-dimensional focal plane arrays (FPAs) by its internal optics. A variety of foreoptics can be used to project the image on the slit, provided that they match the $f/17$ design of the internal optics. (Slower or faster optics may also be used, but their performance is not optimal—slower foreoptics underfill the internal optics and may result in some loss of spectral resolution while faster optics overfill the internal optics and vignette, resulting in the loss of light.) The desired field of view (FOV) along the slit together with the physical length of the slit determine the focal length of the foreoptics. An FOV of $\sim 9^\circ$ was selected, resulting in a foreoptic with an effective focal length of 241.7 mm. The effective focal length together with the $f/17$ constraint of the internal optics of the spectrograph resulted in an entrance pupil diameter of ~ 14 mm. This turned out to be more than ample for the very bright targets that were observed.

Another restriction on the foreoptics was that they produce a telecentric output. This means that entrance pupil appears at infinite distance and results in the necessary condition that the light cones from all locations of the FOV are parallel when incident on the entrance slit of the spectrograph. The latter requirement was imposed by compatibility with the astronomical application for which NIRIS was originally designed. In that case the entrance pupil, which is the telescope primary mirror, is more than 50 meters away—effectively at infinite distance.

The foreoptics were designed with an additional desirable feature, namely a forward pupil. The entrance pupil is located approximately two inches in front of the first optic. This is an ideal location to place a stop to restrict stray light. The neutral density filters and the fast shutter are also positioned there, ensuring that they affect all parts of the FOV uniformly.

The requirements of FOV, wavelength coverage, telecentricity, and forward pupil were met with the three-lens design described in Table 1. Two of the lenses were composed of BaF_2 and were designed to match commercially available units from Janos Optics, Inc. The third lens was a custom design composed of SNPH2, a glass from Ohara, and was fabricated by Kreischer Optics, Inc. The combination of the three lenses and the two different materials provide the chromatic correction necessary to achieve a common focus over the broad wavelength range covered by the spectrograph, and to accommodate the viewing from the reflective slit (which is done at visible wavelengths) as well. Figure 1 shows the lenses within the barrel that holds and maintains their precise orientations and separations. Figure 2 illustrates both the FOV and how a distant point source would be imaged. The internal optics of NIRIS reduce the field image projected on the slit by a factor 6 while re-imaging it onto the detector arrays. This ensures that all points of the field are re-imaged at sizes well under the dimension of a pixel ($18.5 \mu\text{m}$).

Table 1. Code V Description of NIRIS Foreoptic

kelleya.12 test plate fit

	RDY	THI	RMD	GLA
OBJ:	INFINITY	INFINITY		
STO:	INFINITY	71.695868		
2:	112.89000	3.600000		BAF_SPECIAL
3:	INFINITY	49.135069		AIR
4:	66.19200	5.000000		'snph2'
5:	53.42130	128.383072		
6:	INFINITY	5.400000		BAF_SPECIAL
7:	-112.89000	107.130298		
> IMG:	INFINITY	0.000000		

SPECIFICATION DATA

EPD	14.25000				
DIM	MM				
WL	2450.00	2200.00	1650.00	1250.00	850.00
REF	3				
WTW	1	1	1	1	1
XIM	0.00000	0.00000	0.00000		
YIM	0.00000	11.55000	16.50000		

APERTURE DATA/EDGE DEFINITIONS

CA	
CIR S5	17.000000
CIR S2 EDG	19.050000
CIR S3 EDG	19.050000
CIR S4 EDG	19.050000
CIR S5 EDG	19.050000
CIR S6 EDG	25.400000
CIR S7 EDG	25.400000

REFRACTIVE INDICES

GLASS CODE	2450.00	2200.00	1650.00	1250.00	850.00
BAF_SPECIAL	1.463138	1.463961	1.465706	1.467188	1.469834
'snph2'	1.838856	1.845330	1.858518	1.869133	1.887739

INFINITE CONJUGATES

EFL	241.7126
BFL	107.3853
FFL	-5.1694
FNO	16.9623
IMG DIS	107.1303
OAL	263.2140
PARAXIAL IMAGE	
HT	16.5000
ANG	3.9051
ENTRANCE PUPIL	
DIA	14.2500
THI	0.0000
EXIT PUPIL	
DIA	666.3055
THI	-11194.6788

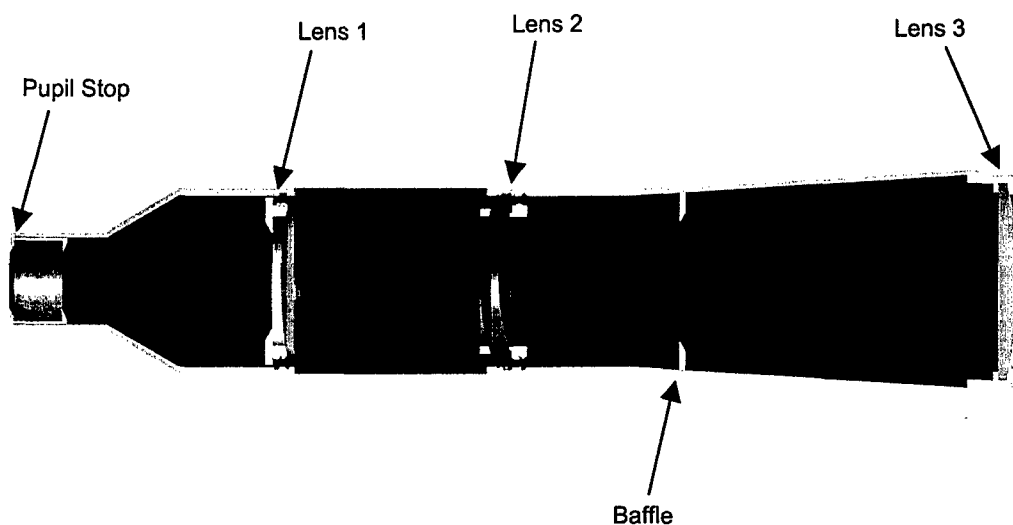


Figure 1. 9° FOV telescope that serves as the foreoptic for the NIRIS spectrograph. The three lenses that form the telescope are held by two separate cylinders that thread together. A third threaded section (at the left side of the figure) supports a stop at the location of the entrance pupil that defines the entrance pupil and reduces the scattered light. The above structure is 27 cm in length.

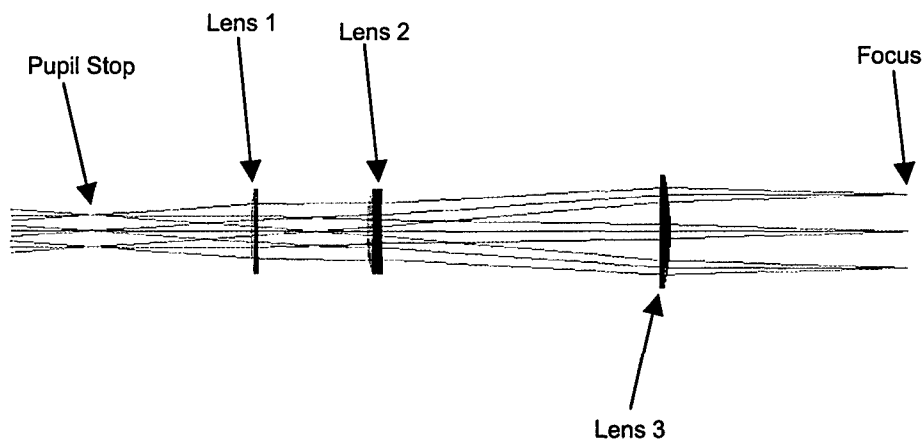


Figure 2. Cut-away view of the telescope demonstrating its function. Light enters from the left over a 9° FOV. Green rays represent points at the boundary of the field of view. A central red cylinder represents the light from a distant point source at the center of the FOV. This is focused by the telescope at the extreme right side of the view (along with all other points within the FOV) at the position of the spectrograph entrance slit. If the full pupil is illuminated, the convergence cone matches the $f/17$ design of the internal optics of the spectrograph.

3. Mechanical Design

The mechanical design effort was divided into two main categories, one was to precisely mount the three lenses that comprise the foreoptics with the orientations and spacings specified by the optical design. The second was to attach NIRIS and its foreoptics, cameras, filterwheel, fast shutter, etc. to the tracking mount.

The mounting of the three lenses was accomplished using the tube-like structure expected for the all-refractive design. This has been shown above in Figures 1 and 2.

Attachment of the spectrograph to the tracking mount was accomplished with a large G-10 (fiber-glass) plate. G-10 was chosen both for its strength and its electrical insulating properties, the latter being critical for isolating the sensitive analog signals from the large currents circulating in the tracking mount. The plate also served as an optical bench of sorts, allowing for the positioning of the shutter and filterwheel immediately in front of the foreoptic telescope, and the attachment of the video and slit-viewing cameras. Figures 3 and 4 illustrate the full experimental set-up, and Figures 5 and 6 show the placement of the experimental equipment on the cine-sextant tracking mount.

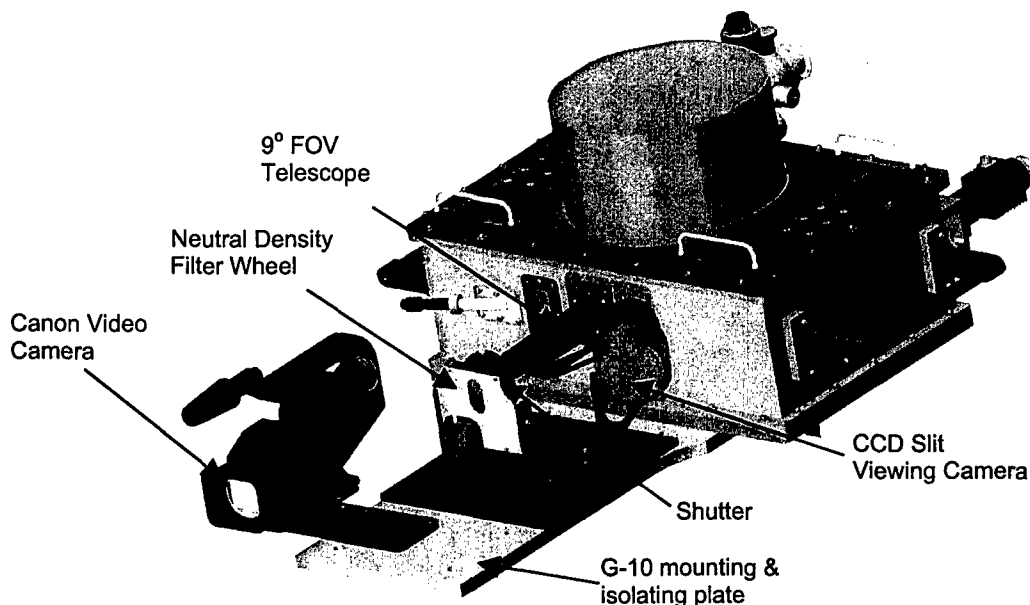


Figure 3. The NIRIS spectrograph (gold structure) together with the supporting equipment used to adapt NIRIS for hyperspectral imaging of rocket plumes. The telescope has a small aperture (14 mm dia) and a large field of view (9°). It is preceded by a filterwheel with a selection of neutral-density filters (for signal attenuation) and a fast shutter (also for signal attenuation). The telescope images the FOV on the entrance slit of the spectrograph, which passes a slice of the image on to the internal optics. The remainder of the FOV is reflected by the slit jaws to the slit-viewing CCD camera. This camera takes a snapshot of the surrounding field when a hyperspectral image is captured. For continuous monitoring of the target and the surrounding field, a video camera is also provided. It is attached to an azimuth/elevation mount for co-alignment with the spectrograph's foreoptic telescope.

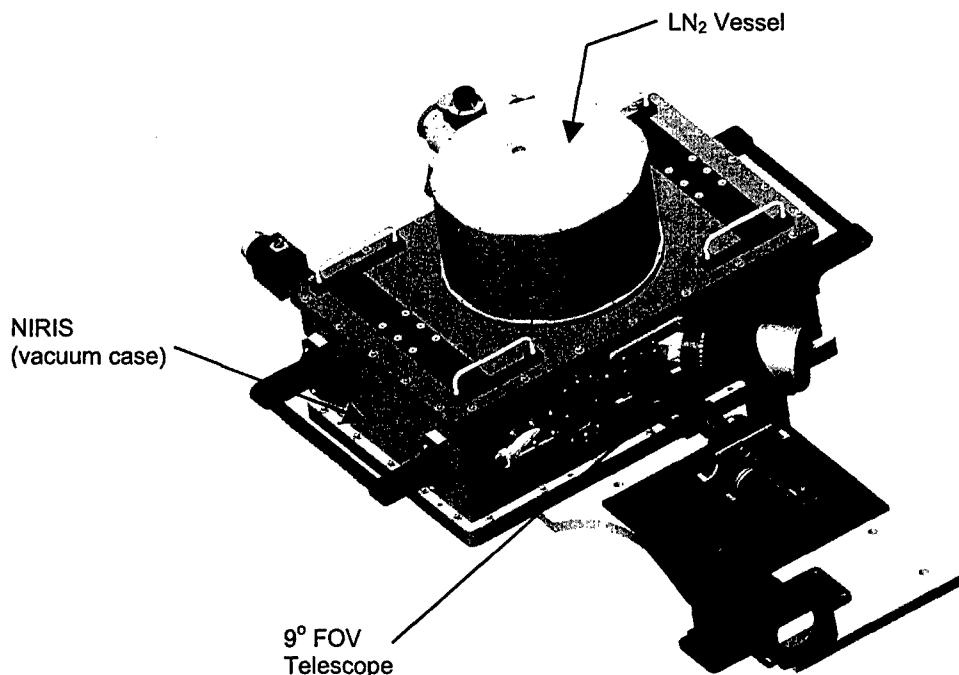


Figure 4. A second view of the instrument setup. For scale, the width of the spectrograph is 31.5 in. The LN₂ vessel accommodates 6.7 liters of liquid nitrogen that provides for the cooling both the focal-plane arrays (to 82 K) and the infrared optics (to 140K).

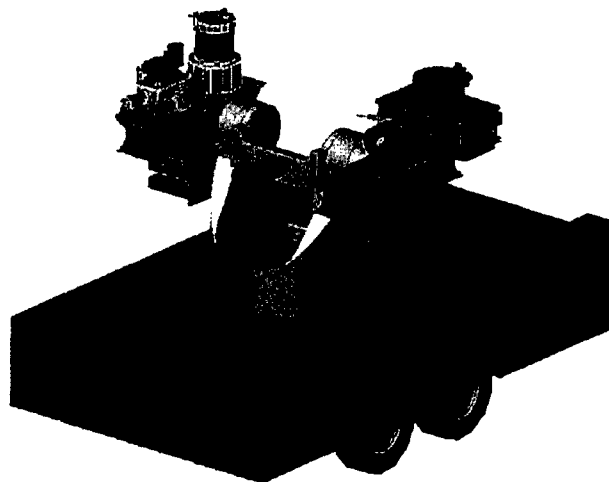


Figure 5. Simplified scale drawing of cine-sextant mount with NIRIS spectrograph. The cine-sextant mount from Photo-Sonics International provides rapid alt-azimuth slewing and tracking and was provided by launch support at Vandenberg Air Force Base. One arm of the mount was devoted to NIRIS and its attendant equipment; the second arm supported other instrumentation from The Aerospace Corporation's Remote Sensing Department. The horizontal tube-like structure facing left at the center of the mount is the operator's telescope. The mount is towed to the observing location. The Photo-Sonics cine-sextant mount requires an external generator to supply 220 V, 3-phase power for operations. While some cine-sextant mounts contain a GPS receiver for timing and geo-location, the unit employed for the Titan observations was not so equipped. An external GOES timing receiver was used to generate IRIG timing signals to time-stamp the video signal from the NIRIS FOV camera.

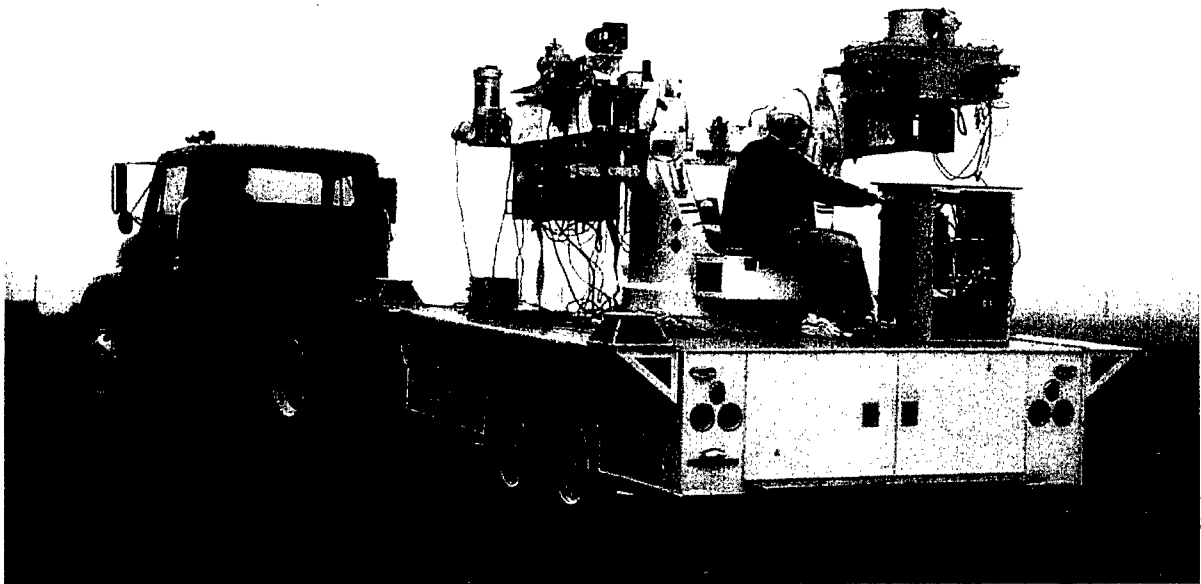


Figure 6. The NIRIS spectrograph installed on the Photo-Sonics cine sextant tracking mount as it is being towed to its observing site at Vandenberg Air Force Base. NIRIS is the instrument in the upper right—additional IR cameras and spectrographs are mounted on the left arm of the mount. The site is approximately 4.8 km from the Titan II space launch complex.

4. Electronics and Data acquisition

The electronics and data acquisition system consist of a blend of custom and commercially available electronics. Figure 7 shows a block diagram of experimental set-up, including the communication links among components. The preponderance of the custom electronics, termed GenCam (for Generic Camera) and developed by the Space Instruments Department, is concerned with the operation of the FPAs. The clocks that are necessary to reset and read-out the arrays are generated by a microsequencer. A compiler provides the interface necessary to translate simple ASCII commands into machine language. Once compiled, a selection of clock sequences, corresponding to different data acquisition modes, can be downloaded to the microsequencer from the data acquisition computer. Once downloaded, the microsequencer will repeat the clock pattern until commanded to stop. The analog signals from the two outputs of each FPA are boosted by individual amplifiers and then passed to dedicated 16-bit analog-to-digital converters (ADCs). After digitization, the signals are transmitted over fiber optics to the separate PC that hosts a Digital Signal Processor (DSP) card. The DSP concatenates the digital streams, performs some simple arithmetic on the 1 megapixels that constitute a full hyperspectral image, and passes the numbers to the computer memory for transfer, via ethernet, to the data acquisition computer. In addition to its other functions, the data acquisition computer provides a display of the raw hyperspectral data image and writes the image to disk. The disk is shared such that the data can be accessed by a separate, data-analysis computer. The data-analysis computer also provides for a quick-look capability.

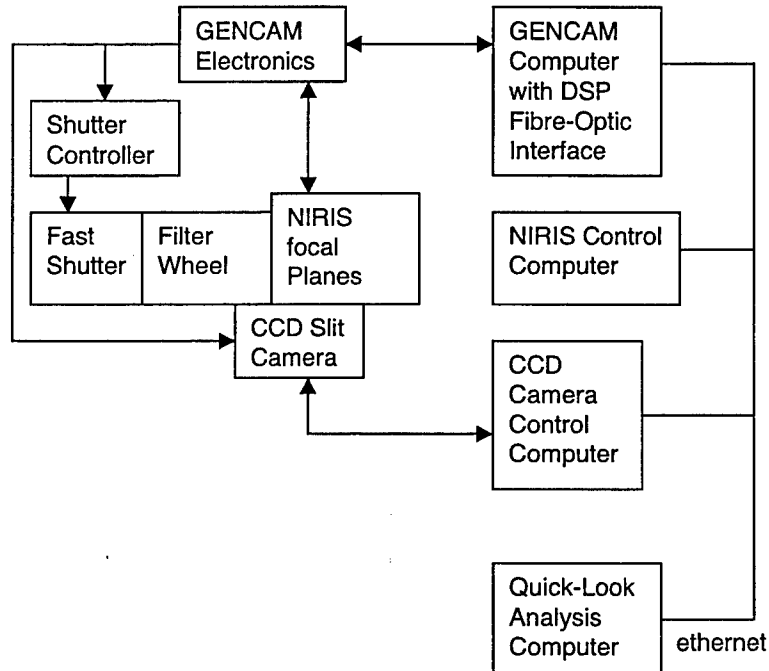


Figure 7. Block diagram showing the key experimental equipment, the control and data acquisition computers, and the connectivity among the components.

In order to improve the rate at which hyperspectral images are obtained, data acquisition modes exist that read only a portion of the FPAs. The full spectral range of the array (distributed along columns) is always read, but it is frequently the case that the target covers only a portion of the FOV. For example, a 100-m target at a distance of 4 km would only subtend about 1.5° . In such a case, it is necessary to read only a fraction of the total number of rows of the array. In practice, we read fractions of the 512 total spatial rows in groupings divisible by two (i.e., 256, 128, 64) so for the 100-m target at 4 km, we would typically observe 128 rows. This ensures complete coverage of the target with margin for guiding errors as well as adequate sampling of the background.

In addition to operating the FPAs, the microsequencer also provides a clock signal that is used to trigger the shutter. The FPAs in NIRIS were fabricated for detection of faint signals. They are low-noise, small-well ($\sim 10^5$ electrons per pixel) devices with comparatively slow frame rates. Thus, the use of shutter is crucial, both to reduce the light to manageable levels and to freeze the image during the long readout procedure. The shutter is a standard Uniblitz model with a 14-mm aperture. Both the shutter and its operating electronics were provided by Vincent Associates, Inc. The duration the shutter was opened for the actual data collects varied between 10 and 15 ms, but times as short as 5 ms are possible.

Although the shutter provides over a factor of 20 reduction in signal levels, this was insufficient to keep the FPAs out of saturation. For this reason, a 6-position filterwheel manufactured by CVI, Inc. and implemented with a selection of neutral-density filters was added to the optical train. Densities of 1.0, 1.5, 2.5, and 3.0 (reductions of 10, 31.6, 316, and 1000, respectively) as well as unfiltered positions were included. The neutral-density filters were fabricated in the coatings facilities resident in The Aerospace Corporation's Laboratory Operations. The filterwheel is not currently under computer control.

5. Supplementary Imaging

Although NIRIS is a hyperspectral instrument, it has proved extremely useful while observing a launch to have synchronous visible imaging. This is accomplished both by a video camera that views the launch vehicle directly, and by a separate camera that uses the NIRIS telescope and directly images the entrance slit of NIRIS. Although the jaws that form the entrance slit of NIRIS are mounted to flexures and spread by a linear actuator like a conventional spectrograph, they are also reflective and angled slightly to line-of-sight. Light not passing through the slit and into the spectrograph is reflected through an exit window to a camera that is focused on the slit. This provides a simultaneous view of the slit and the field surrounding the slit, yielding an exact view of what is observed (see Figure 8). To accommodate the low light levels that resulted

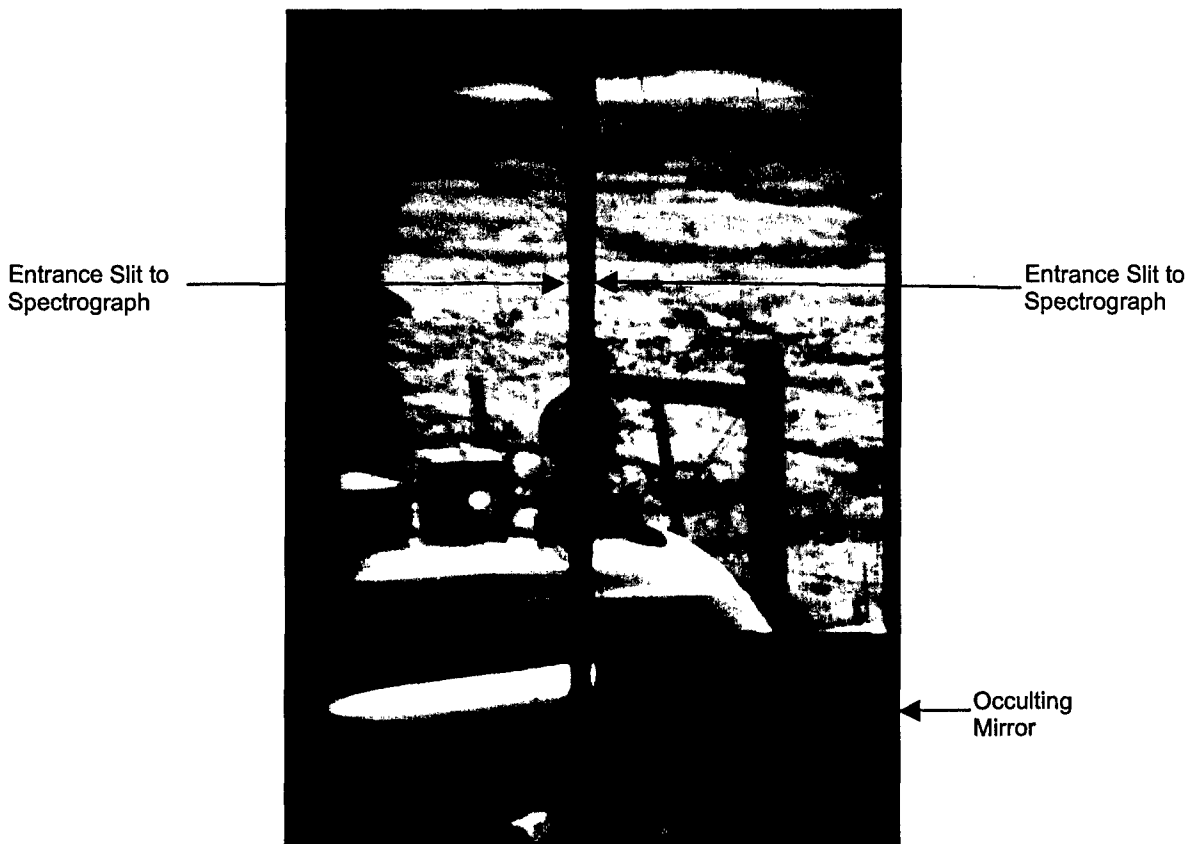


Figure 8. Image from the slit viewing CCD. The two opposed arrows show the entrance slit to the spectrograph (i.e., the dark vertical strip). On both sides of the slit, the jaws reflect an image of the surrounding scene. This particular image was acquired during calibration. The cylindrical object centered on the slit and about half way between top and bottom is a cavity blackbody. The square object to the left is also a blackbody; the very bright emit-tance from its aperture is the bright circle. Both blackbodies are sitting on a cargo van; a fence post is to the right of the blackbody in the background; and the horizon can be seen at the very top of the image. The occulting mirror allows for observing a faint source near a very bright one and is not utilized for launch observations.

from the very short exposure times (10–15 ms) and the neutral-density filters, a low-light-level, cooled CCD is used that is triggered by the microsequencer and synched to the shutter. The CCD has its own dedicated shutter to reject any stray daylight that may enter the optical train. The microsequencer provides a pulse to open this shutter 10 ms before the master shutter is activated. This ensures that the CCD shutter is fully open when the actual data collection begins. The use of the slit camera provided accurate monitoring of the tracking of the rocket.

To observe the entire field of view around the launch vehicle, the experimental set-up also includes a Canon model XL1s video camera. The Canon XL1s camera uses a 3 CCD system to capture full-color video images. An internal prism separates the light into the primary colors for projection onto individual CCD chips, allowing for accurate registration and high sensitivity. The CCDs use 72- μm square pixels (8.5- μm pixel pitch). In addition, the XL1s allows for the use of interchangeable lenses so that we can adapt the focal length to meet observing conditions. For the Titan observations, we employed a 400-mm Canon EF series fixed-focus lens, in conjunction with a n EF adapter to mount the lens to the XL1s. A series of images from the Titan II DMSP launch of 18 October 2003 are shown in Figures 9–11. The EF adapter increases the image magnification by a factor of 7.2, resulting in an effective focal length of ~ 2800 mm. The output video signal from the XL1s camera was routed through a video timecode generator to insert a timecode into each frame. The timecode was generated using an IRIG (Inter-Range Instrumentation Group) signal provided by a GOES (Geostationary Operational Environmental Satellite) time receiver. Video data were then digitized and recorded direct to disc using a Macintosh computer, with a VHS recorder running in parallel as backup. The use of the computer to record the data in real time eliminated the degradation that would have been introduced by digitizing from a tape recording as we had done on previous field observations. Direct recording also allowed for rapid post-launch analysis of the video in conjunction with the NIRIS data.

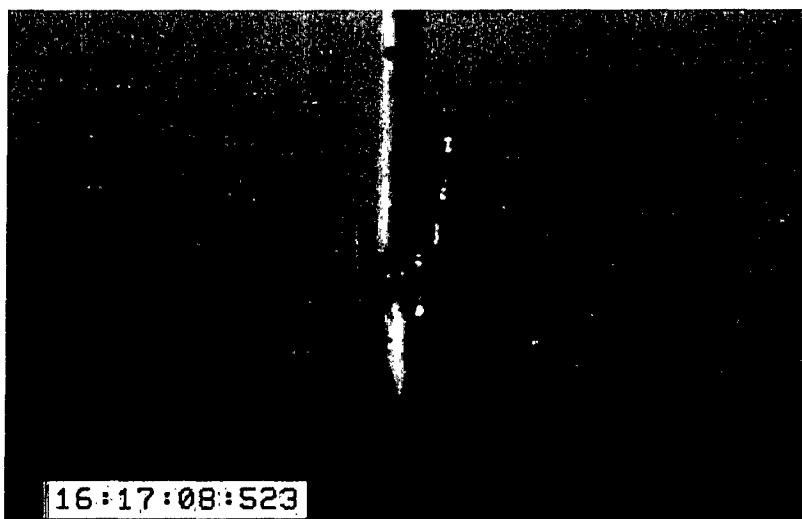


Figure 9. Titan II DMSP Launch from October 18, 2003 at Vandenberg Air Force Base. This image was acquired with the Canon XL1s video camera that is bore-sighted in the same direction as the spectrograph telescope. The image is from a few seconds after ignition as the rocket is about to clear the tower. The horizon and a set of telephone lines are in the foreground. Some noise pickup from the large electric motors of the tracking mount are present in the image. The launch pad is 4.8 km from the observation locale. The very useful time stamp was provided by routing the output video signal through a video timecode generator.



Figure 10. Image of Titan II DMSP from 25 s after liftoff.

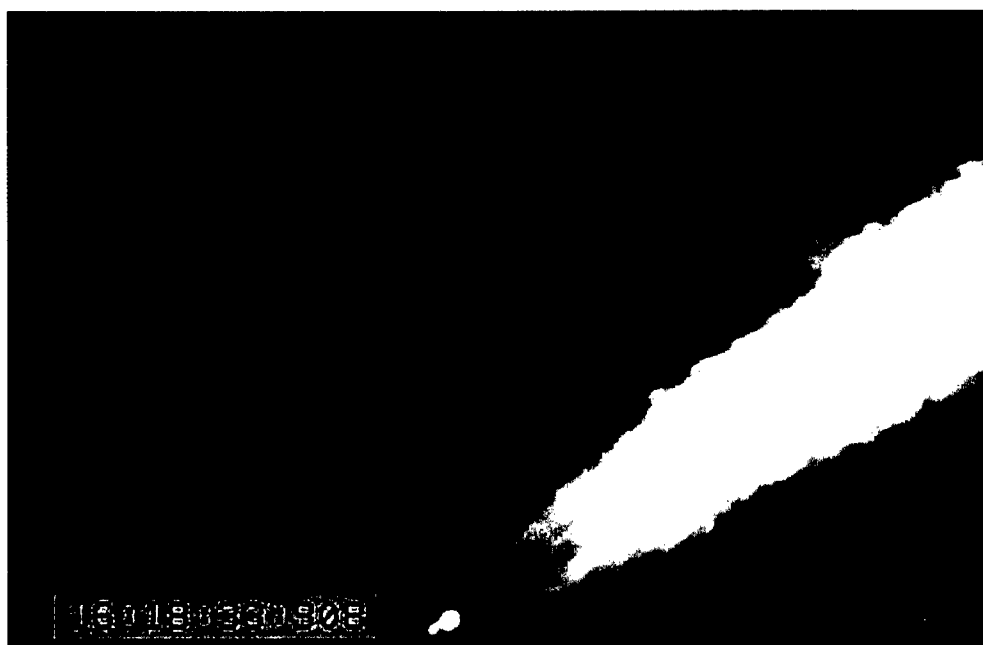


Figure 11. Image of Titan II DMSP from 90 s after liftoff. The vehicle is far downrange, but is still detectable by the spectrograph.

6. Calibration

Because luminosities are critical to the characterization of plume processes as well as good spectra, there has been a concerted effort to acquire accurate spectrophotometry as well as good relative spectroscopy. The method applied to accomplish this is to include observations of cavity blackbodies before and after launch, and in the laboratory prior to deployment. Cavity blackbodies use a shaped cavity with a small opening to achieve an emissivity within a few tenths of a percent of unity. This effectively removes the emissivity as a variable and results in an emittance that is described accurately by the Planck function. The temperature then becomes the only parameter determining the spectral energy distribution of the emittance, and it is measured independently from the blackbody controller, a calibrated thermocouple, and an infrared thermometer. This combination typically results in an error of only $\pm 4^\circ$ for a nominal temperature of 1000°C . This translates into an uncertainty of $<5\%$ in the radiance at our shortest wavelengths. The quoted uncertainty in the absolute calibration, $\pm 20\%$, is considerably larger than this and reflects differences in color temperature between the blackbody and rocket plume, the very different distances at which the two sources are observed, and small instrument variations due to the different orientations of the spectrograph at which the sources are measured.

7. Performance Capabilities

Table 2 summarizes the spectrograph performance parameters and capability. Values are all for the 9° FOV, 14-mm foreoptic described in Section 2. Figures 12 and 13 illustrate the capability with some spectra acquired from Vandenberg Air Force Base.

Table 2. Summary of Instrument Parameters and Capabilities

- Wavelength Coverage: 0.8–2.5 μm (two individual channels)
 - Blue channel: 0.8–1.4 μm
 - Red channel: 1.4–2.5 μm
- Spectral Resolution ($\lambda/\Delta\lambda$)
 - Blue channel: 700–1200
 - Red channel: 560–1000
- FPAs: two 1024 x 512 HgCdTe—1024 spectral, 512 spatial
- FOV: 9° along the slit—785 m at 5 km
- IFOV: 0.46 mr—2.3 m at 5 km
- FOV (across slit): up to 4.1 mr—20.5 m at 5 km
- FOR (on Cine-Sextant Mount): Azimuth $\pm 90^\circ$, Elevation 0–90°
- Aperture Diameter (light gathering): 14.25 mm
- Frame Rate: up to 3.25 Hz if 1024 x 128 subframes taken for each channel
- Cooling: LN_2
- Supplementary Imaging:
 - Slit Camera
 - Video Camera: Canon Model XL1s

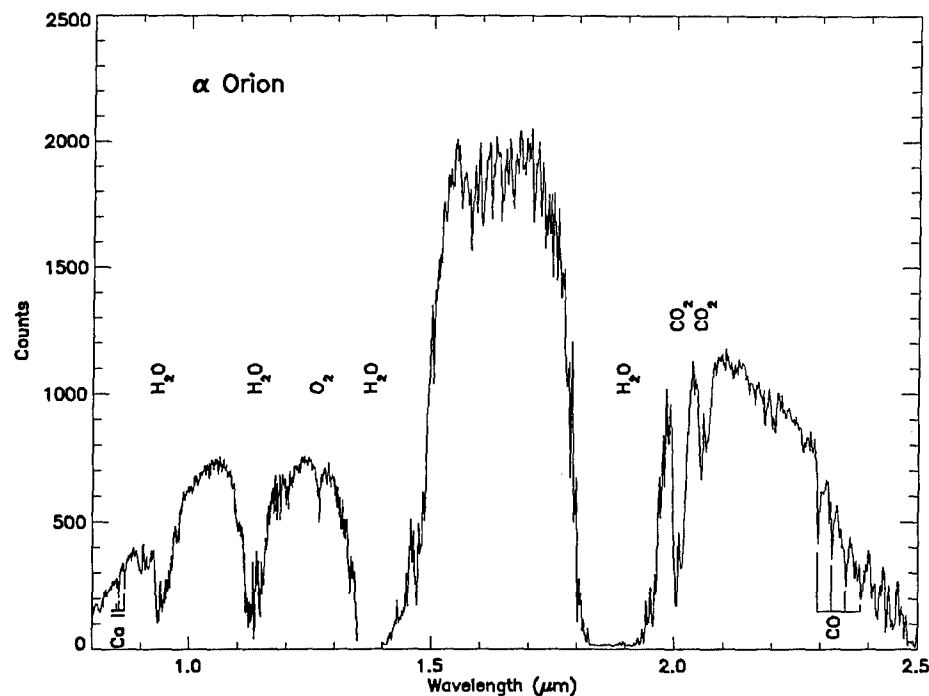


Figure 12. Spectrum of the bright infrared star α Orionis acquired shortly before sunrise on the morning of Oct 18, 2003 from Vandenberg Air Force Base. The data were obtained using the same equipment employed for the observations of the Titan II DMSP launch later that morning, including the 1-cm-dia telescope. The labels above the spectrum refer to absorptions due to the Earth's atmosphere; those marked below, most notably the strong first overtone emission of carbon monoxide, are intrinsic to the star.

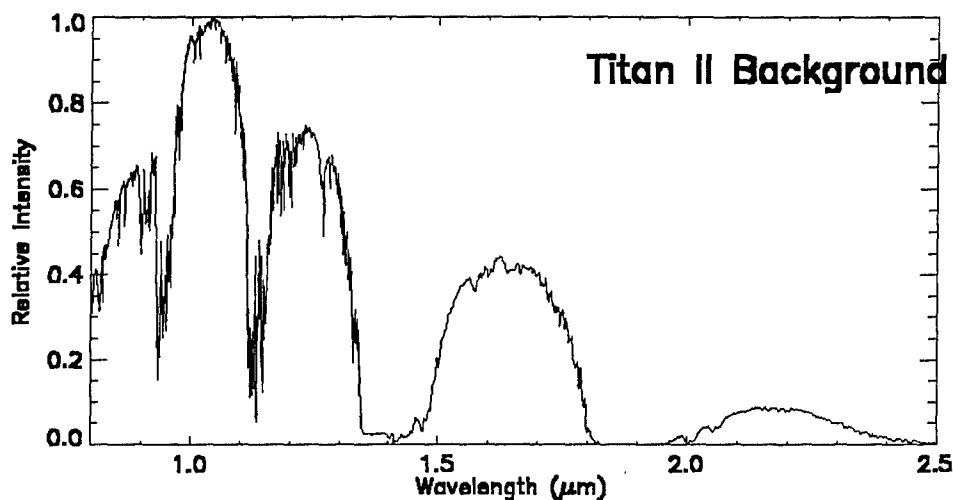


Figure 13. Spectrum of sunlit sky from shortly after the Titan II NOAA launch. Like the stellar source α Orionis, the spectrum is dominated by telluric absorption features. The sun is a hotter star than α Orionis, however, and manifests different features. Because of the higher temperature, carbon monoxide is very weak in the sun, but the lines of atomic hydrogen are much stronger. The most prominent H I lines in the above spectrum are the Paschen series lines Pa β (1.2818 μ m), Pa γ (1.0938 μ m), and Pa δ (1.0049 μ m). The near-infrared Ca II triplet is strong in both α Orionis and the sun

8. Summary and Future Upgrades

This document has described the modifications and augmentations necessary to adapt a hyperspectral instrument developed originally for observations of faint, static sources to the measurement of bright, rapidly varying rocket plumes. This was accomplished by (1) providing a foreoptic for the spectrograph to image the field of interest on the spectrograph entrance slit, (2) by reducing the intensity of the scene through use of neutral-density filters and a fast shutter, (3) by windowing the spectrograph focal planes to sample only the hyperspectral scene of interest, and (4) by mounting the spectrograph to a tracking mount that is capable of following the launch vehicle from liftoff through flight.

Two upgrades are underway that can be utilized in future observations. The first is the development of an additional channel for the spectrograph that extends its capability into the visible (0.4–0.9 μm). This channel uses the same foreoptic and same entrance slit as the existing infrared channels. The second upgrade is the fabrication of an additional foreoptic, in this case a 10-in.-dia Cassegrain telescope that is also matched to the f-number of the spectrograph optics. It provides much greater light gathering power (although over a much smaller field of view [0.5°]) and can be used for observations from a greater initial distance and to follow the vehicle much further down range.



2350 E. El Segundo Boulevard
El Segundo, California 90245-4691
U.S.A.